

Overheated Topological Hall Effect: How Possible Artifacts Emerge?

Liang Wu^{1, a)} and Yujun Zhang²

¹⁾*Faculty of Materials Science and Engineering, Kunming University of Science and Technology, Kunming Yunnan, 650093 China.*

²⁾*Institute of High Energy Physics, Chinese Academy of Science, Yuquan Road 19B, Shijingshan District, Beijing, 100049 China*

(Dated: 2 September 2020)

Topological Hall effect (THE) originates from the real-space Berry phase that an electron gains when its spin follows the spatially varying non-trivial magnetization textures, such as skyrmions. Such topologically protected magnetization textures can provide great potential for information storage and processing, which spurs a new wave of THE research. Since directly imaging the skyrmions or detecting the magnetic diffraction of skyrmion lattice are more challenging than conducting Hall measurements, THE has been widely used to attest the presence of skyrmions. However, as the key feature of THE, the bump/dip in Hall signal is not a sufficient proof of THE [Phys. Rev. B. **98**,180408(2018) and Phys. Rev. B. **98**, 214440(2018)]. Here, we use empirical numerical modeling to demonstrate all possible THE-like signals that two anomalous Hall effect (AHE) signals with opposite signs can superpose. We accentuate that similar Hall signals observed in experiments require scrupulous re-examination to claim the advent of THE and related skyrmions. In addition, the origin of two-channel AHE in several representative examples are also been analyzed.

The concept of Berry phase has been deeply rooted in the modern condensed matter physics, which reveals the role of momentum-space topology in various observable novel effects. The quintessential examples are those notable members in the Hall family, such as quantum Hall effect and anomalous Hall effect (AHE)¹. Recently, the topology of the non-trivial spin texture in real space was found to contribute a non-vanishing Berry phase as well, whose effect on the transverse motion of electrons was dubbed as topological Hall effect (THE)². To date, the widely-accepted criterion of the presence of THE is the additional bumps/dips along with the AHE. However, this would be no longer sufficient when there exist multiple conduction channels with opposite AHE signs^{3,4}. In this letter, numerical modeling was utilized to extend and generalize the results of reference [3-4] and simulate all possible situations of two superposed AHE signals with a comprehensive summary of the previously published results. We underline that THE-like Hall signals should be taken more seriously when claiming the existence of THE and related skyrmions.

A. Numerical modeling

THE-like Hall signal can be mimicked by superposition of two AHE signals with opposite signs. Similar to the magnetization versus field hysteresis, an empirical model of $R_{\text{AHE}}^{\text{I}} = M_{\text{I}} \tanh(\omega_{\text{I}}(H - H_{\text{c}}^{\text{I}}))$, can be used to model the AHE signals, where M_{I} , ω_{I} and H_{c}^{I} stand for the AHE magnitude, slope parameter at coercive field and coercive field. An additional AHE channel can be represented as $R_{\text{AHE}}^{\text{II}} = M_{\text{II}} \tanh(\omega_{\text{II}}(H - H_{\text{c}}^{\text{II}}))$. Thus the overall AHE can be presented by the following equation,

$$R_{\text{AHE}}^{\text{tot}} = M_{\text{I}} R_{\text{AHE}}^{\text{I}} \tanh(\omega_{\text{I}}(H - H_{\text{c}}^{\text{I}})) + M_{\text{II}} R_{\text{AHE}}^{\text{II}} \tanh(\omega_{\text{II}}(H - H_{\text{c}}^{\text{II}})) \quad (1)$$

To simplify the discussion, we set $M_{\text{I}} > 0$ and $M_{\text{II}} < 0$ to ensure the two channels are of opposite signs. Thus, the characteristic shape of the overall AHE would only be affected by the relative magnitude of these parameters. By exhaustive enumeration, we systematically studied all four cases with (a) $|M_{\text{I}}| = |M_{\text{II}}|$ and $\omega_{\text{I}} = \omega_{\text{II}}$, (b) $|M_{\text{I}}| = |M_{\text{II}}|$ and $\omega_{\text{I}} \neq \omega_{\text{II}}$, (c) $|M_{\text{I}}| \neq |M_{\text{II}}|$ and $\omega_{\text{I}} = \omega_{\text{II}}$, (d) $|M_{\text{I}}| \neq |M_{\text{II}}|$ and $\omega_{\text{I}} \neq \omega_{\text{II}}$, by varying the relative magnitude of their coercive fields H_{c} , as shown in Fig. 1. Without loss of generality, here we set $|M_{\text{I}}| > |M_{\text{II}}|$ for $|M_{\text{I}}| \neq |M_{\text{II}}|$, which indicates the magnitude of AHE for channel I is larger than that of channel II. While we set $\omega_{\text{I}} < \omega_{\text{II}}$ for $\omega_{\text{I}} \neq \omega_{\text{II}}$, which means channel II has a steeper transition than channel I near H_{c} .

As immediately seen in Fig. 1, the THE-like bumps/dips can generally be generated in all cases. From experimental point of view, Hall signals similar to a_{34} , b_{24} , c_{23} , and c_{24} are widely observed and explained by references^{3,4} and many of them are listed in Table I. Special cases like d_{11} can be found in references⁵⁻⁸, representing the situations of negligible H_{c} (eg. superparamagnetic or ferromagnetic near Curie temperature), which can be understood by reference⁴. While similar putative THE like d_{22} has been found recently in LaMnO₃/SrIrO₃ heterostructure⁹. In addition, we also predict a novel Hall signal similar to b_{33} , representing the situation with difference only in ω of the two channels, which has not been experimentally observed yet.

To summarize, the hysteresis behaviors of the previously published THE results can generally be imitated by two superposed AHE hysteresis as shown Fig. 1. To offer a deeper understanding, we next discuss the possible origin of the two-channel AHE signals.

^{a)}Electronic mail: liang-wu@kust.edu.cn

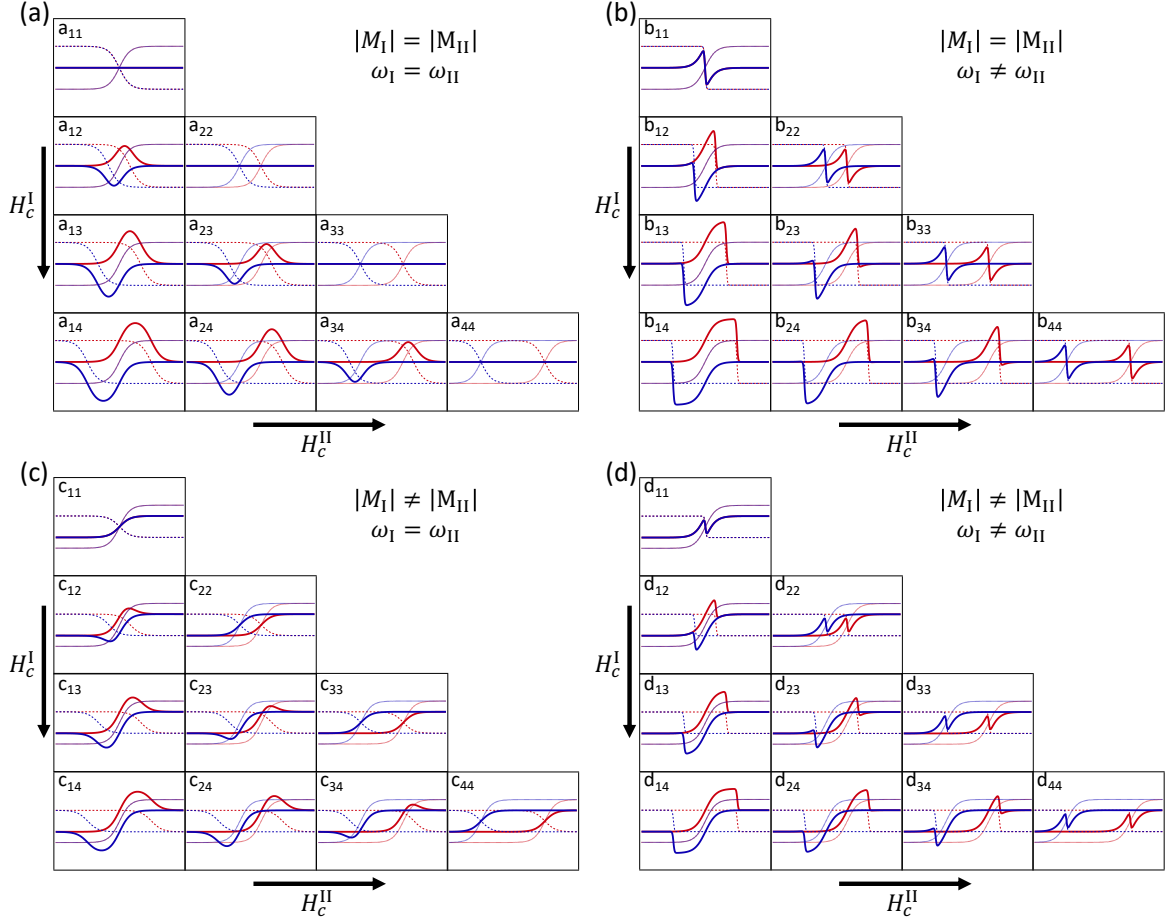


FIG. 1. **Numerical modeling of the superposition of two opposite AHE signals.** The dotted, dashed and solid lines represent the positive, negative and total Hall channels, respectively. The colors indicate the directions of field sweep (red: increase, blue: decrease). The arrows indicate the increasing of H_c . (a) $|M_I| = |M_{II}|$ and $\omega_I = \omega_{II}$, (b) $|M_I| = |M_{II}|$ and $\omega_I \neq \omega_{II}$, (c) $|M_I| \neq |M_{II}|$ and $\omega_I = \omega_{II}$, (d) $|M_I| \neq |M_{II}|$ and $\omega_I \neq \omega_{II}$.

B. The origin of two-channel AHE

Since the AHE is both sensitive to the intrinsic electronic structure near the Fermi level and extrinsic sample inhomogeneity, the coexistence of two opposite AHE channels could occur in many materials and heterostructures. As for the intrinsic properties, the multiple Weyl nodes with opposite signs of Berry curvature can induce the bump/dip in the resultant Hall signal, such as $(\text{Bi}_{1-x}\text{Mn}_x)_2\text{Se}_3$ ¹⁰ and EuTiO_3 ¹¹. On the other hand, as thickness, temperature, doping, electrical gating etc. can induce the AHE sign reversal, an inhomogeneous sample with a corresponding broadening sign reversal range could naturally give rise to a Hall signal mimicking THE features. In addition, heterostructures may contain opposite AHE signals at different interfaces to induce a THE-like Hall.

For instance, SrRuO_3 shows a sign reversal at a critical thickness of 4 unit cell (u.c.). Even one u.c. thickness fluctuation can blend the positive AHE from 4 u.c. and negative AHE from 5 u.c. (or thicker regions) to induce the bump in Hall signal in a nominal 4 or 5 u.c. sample¹² (See Fig. 2a).

SrRuO_3 also possesses a temperature dependent AHE sign reversal. We can assume there exists two spatial regions with different critical temperatures, T_1 and T_2 ($T_1 < T_2$) in an inhomogeneous SrRuO_3 . In the temperature range between T_1 and T_2 , two opposite AHE signals would appear and mix with each other³ (See Fig. 2b) to give rise to the THE-like overall Hall signal. It is worth noting that, in this case, the THE-like Hall signal can only occur in the temperature range of T_1 and T_2 , because for $T < T_1$ or $T > T_2$, the two-channel AHE signals are of the same sign.

Thus, typical published THE materials can be classified by the existence of AHE sign reversal and listed in Table I. Note that due to the limit of our knowledge and the huge number of publications in THE, this table is not able to give a exhaustive list. We stress that the observed bump/dip, especially in the systems with AHE sign reversal, should be treated extremely carefully to determine it is the effect of the intrinsic Berry phase or extrinsic sample inhomogeneity.

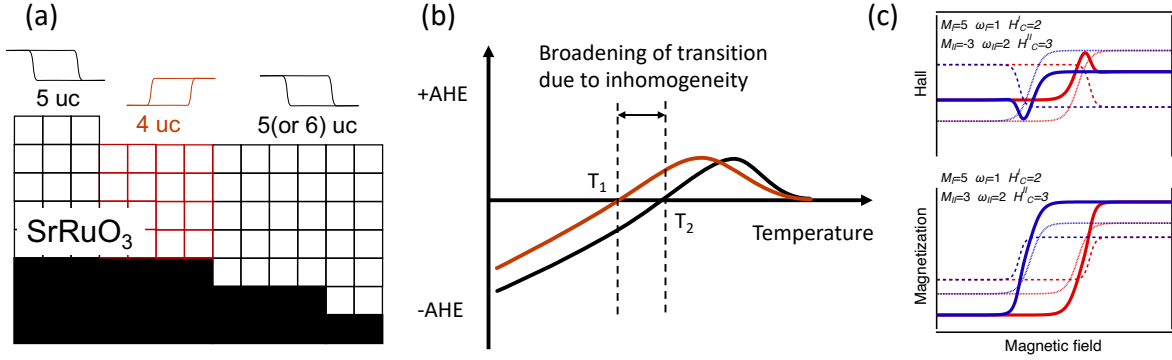


FIG. 2. Coexistence of two opposite AHE channels induced by synergistic effects of (a) thickness fluctuation and thickness-dependent AHE sign reversal, (b) sample inhomogeneity and temperature-dependent AHE sign reversal. Only in the temperature range of T_1 and T_2 , THE-like Hall signal appears. (c) Modeling of two-channel AHE and MH, where bump/dip can be seen in Hall, while two-step transition is not shown in MH loops due to the similarity of ω and H_c of the two channels.

TABLE I. Classification of the previously published THE materials with the sign reversal of the concurrent AHE

THE in AHE sign reversal systems	
Temperature-dependent AHE reversal	SrRuO ₃ ^{8,13-17} , MnGe ¹⁸ , Cr _x (Bi _{1-y} Sb _y) _{2-x} Te ₃ /(Bi _{1-y} Sb _y) _{2-x} Te ₃ ¹⁹ , (Bi _{1-y} Sb _y) _{2-x} Te ₃ /MnTe ²⁰ , CrTe ²¹ , Mn ₂ CoAl ²² , MnGa/Pt(or Ta) ²³ , Bi-Cr ₂ Te ₃ ²⁴ , LaMnO ₃ /SrIrO ₃ ⁹
Thickness-dependent AHE reversal	SrRuO ₃ ^{13-15,25} , CrTe ²¹
Gating-dependent AHE reversal	SrRuO ₃ ²⁶ , Sb ₂ Te ₃ /V doped Sb ₂ Te ₃ ⁸
Doping-dependent AHE reversal	Mn _{1-x} Co _x P ²⁷
THE without or indetermination of AHE sign reversal	(Bi _{0.9} Mn _{0.1}) ₂ Te ₃ ²⁸ , MnSi ¹⁸ , Pt/Cr ₂ O ₃ ⁶ , Pt/Tm ₃ Fe ₅ O ₁₂ ^{5,7} , Gd ₂ PdSi ₃ ²⁹ , Ca _{1-x} Ce _x MnO ₃ ³⁰

C. Approaches to distinguish THE and two-channel AHE

From the aforementioned discussion, other than the Hall measurements, additional methods are necessary to distinguish THE and two-channel AHE. To predicate a real THE, reliable methods to directly image the spin textures like skyrmions are neutron scattering in momentum space³¹⁻³³ and lorentz electron microscopy techniques in real space³⁴⁻³⁶ and spin-resolved scanning tunnelling microscopy³⁷. Other magnetic domain resolved methods, such as magnetic force microscopy (MFM), magneto-optical Kerr effect (MOKE), photoemission electron microscopy (PEEM), can hardly distinguish the topologically trivial magnetic bubble and non-trivial spin textures. The trivial magnetic bubbles^{38,39} have zero winding number, which will make no contribution to THE. On the other hand, if a material can be proved absence of AHE sign reversal, a THE-like Hall should be real and originate from non-trivial spin textures.

To witness the two-channel AHE is to identify possible sample inhomogeneity. For instance, MFM can be used to detect the relative magnitude of magnetization. As for SrRuO₃,

since the 4 u.c. SrRuO₃ shows a weaker magnetism than that of the 5 u.c. or thicker SrRuO₃, different thickness can be mapped by MFM⁴⁰ to demontstrate the thickness fluctuation in SrRuO₃. Another hint to dertermine the sample inhomogeneity is the two-step transition MH or magnetoresistance (MR) loops in a inhomogenous magentic sample¹². It is worth highlighting that the bump/dip induced by two-channel oppoiste AHE is highly sensitive to the their ω (slope parameter) and H_c . However, on the contrary, a two-step transition of MH (MR) will not be distinguishable when the differences between of their ω and H_c are small as the two-channel MH (MR) are of the same sign (see Fig. 2c). In addition, the universal scaling relation¹ between anomalous Hall conductivity σ_{AHE} and longitudinal conductivity σ_{xx} can also used to verify the nature of the bump/dip in Hall signal. This is because a real THE is a result of real-space spin topology, which theoretically will not affect the scaling relation solely determined by the AHE component at a high field. Otherwise, the superposed overall AHE of two-channel opposite signal is expected to deviate the scaling relation, which can be seen when the opposite signal is of comparable magnitude, featured by a small

overall AHE with large bump/dip¹².

D. Conclusion

As a newly prominent field, dedicated efforts have been devoted to the study of THE. However, the authenticity of THE has long been overlooked. We argue that different forms of THE can be imitated with tricky two-channel opposite AHE, which is a natural result in inhomogeneous AHE sign reversal systems. Besides the observation of bump/dip in Hall measurements, additional characterizations are demanded to claim the advent of THE and related non-trivial spin textures.

Data Availability Statement

The data that support the findings of this study are available from the corresponding author upon reasonable request.

- ¹N. Nagaosa, J. Sinova, S. Onoda, A. H. MacDonald, and N. P. Ong, "Anomalous Hall effect," *Rev. Mod. Phys.* **82**, 1539–1592 (2010).
- ²P. Bruno, V. K. Dugaev, and M. Taillefumier, "Topological Hall effect and Berry phase in magnetic nanostructures," *Phys. Rev. Lett.* **93**, 096806 (2004).
- ³D. Kan, T. Moriyama, K. Kobayashi, and Y. Shimakawa, "Alternative to the topological interpretation of the transverse resistivity anomalies in SrRuO₃," *Phys. Rev. B* **98**, 180408 (2018).
- ⁴A. Gerber, "Interpretation of experimental evidence of the topological Hall effect," *Phys. Rev. B* **98**, 214440 (2018).
- ⁵Q. Shao, Y. Liu, G. Yu, S. K. Kim, X. Che, C. Tang, Q. L. He, Y. Tserkovnyak, J. Shi, and K. L. Wang, "Topological Hall effect at above room temperature in heterostructures composed of a magnetic insulator and a heavy metal," *Nat. Electron.* **2**, 182–186 (2019).
- ⁶Y. Cheng, S. Yu, M. Zhu, J. Hwang, and F. Yang, "Evidence of the topological Hall effect in Pt/antiferromagnetic insulator bilayers," *Phys. Rev. Lett.* **123**, 237206 (2019).
- ⁷A. S. Ahmed, A. J. Lee, N. Bagues, B. A. McCullian, A. M. A. Thabt, A. Perrine, P. K. Wu, J. R. Rowland, M. Randeria, P. C. Hammel, D. W. McComb, and F. Yang, "Spin-Hall topological Hall effect in highly tunable Pt/ferrimagnetic-insulator bilayers," *Nano Lett.* **19**, 5683–5688 (2019).
- ⁸W. Wang, M. W. Daniels, Z. Liao, Y. Zhao, J. Wang, G. Koster, G. Rijnders, C. Z. Chang, D. Xiao, and W. Wu, "Spin chirality fluctuation in two-dimensional ferromagnets with perpendicular magnetic anisotropy," *Nat. Mater.* **18**, 1054–1059 (2019).
- ⁹E. Skoropata, J. Nichols, J. M. Ok, R. V. Chopdekar, E. S. Choi, A. Rastogi, C. Sohn, X. Gao, S. Yoon, T. Farmer, R. D. Desautels, Y. Choi, D. Haskel, J. W. Freeland, S. Okamoto, M. Brahlek, and H. N. Lee, "Interfacial tuning of chiral magnetic interactions for large topological Hall effects in LaMnO₃/SrIrO₃ heterostructures," *Sci. Adv.* **6**, eaaz3902 (2020).
- ¹⁰N. Liu, J. Teng, and Y. Li, "Two-component anomalous Hall effect in a magnetically doped topological insulator," *Nat. Commun.* **9**, 1282 (2018).
- ¹¹K. S. Takahashi, H. Ishizuka, T. Murata, Q. Y. Wang, Y. Tokura, N. Nagaosa, and M. Kawasaki, "Anomalous Hall effect derived from multiple Weyl nodes in high-mobility EuTiO₃ films," *Sci. Adv.* **4**, eaar7880 (2018).
- ¹²L. Wu, F. Wen, Y. Fu, J. H. Wilson, X. Liu, Y. Zhang, D. M. Vasiukov, M. S. Kareev, J. Pixley, and J. Chakhalian, "Berry phase manipulation in ultrathin SrRuO₃ films," *arXiv preprint arXiv:1907.07579* (2019).
- ¹³J. Matsuno, N. Ogawa, K. Yasuda, F. Kagawa, W. Koshihabe, N. Nagaosa, Y. Tokura, and M. Kawasaki, "Interface-driven topological Hall effect in SrRuO₃-SrIrO₃ bilayer," *Sci. Adv.* **2**, e1600304 (2016).
- ¹⁴L. Wang, Q. Feng, Y. Kim, R. Kim, K. H. Lee, S. D. Pollard, Y. J. Shin, H. Zhou, W. Peng, D. Lee, *et al.*, "Ferroelectrically tunable magnetic skyrmions in ultrathin oxide heterostructures," *Nat. Mater.* **17**, 1087–1094 (2018).
- ¹⁵Q. Qin, L. Liu, W. Lin, X. Shu, Q. Xie, Z. Lim, C. Li, S. He, G. M. Chow, and J. Chen, "Emergence of topological Hall effect in a SrRuO₃ single layer," *Adv. Mater.* **31**, 1807008 (2019).
- ¹⁶K. Y. Meng, A. S. Ahmed, M. Baćani, A. O. Mandru, X. Zhao, N. Bagués, B. D. Esser, J. Flores, D. W. McComb, H. J. Hug, and F. Yang, "Observation of nanoscale skyrmions in SrIrO₃/SrRuO₃ bilayers," *Nano Lett.* **19**, 3169–3175 (2019).
- ¹⁷Y. Gu, Y.-W. Wei, K. Xu, H. Zhang, F. Wang, F. Li, M. S. Saleem, C.-Z. Chang, J. Sun, C. Song, J. Feng, X. Zhong, W. Liu, Z. Zhang, J. Zhu, and F. Pan, "Interfacial oxygen-octahedral-tilting-driven electrically tunable topological Hall effect in ultrathin SrRuO₃ films," *J. Phys. D: Appl. Phys.* **52**, 404001 (2019).
- ¹⁸N. Kanazawa, Y. Onose, T. Arima, D. Okuyama, K. Ohoyama, S. Waki-moto, K. Kakurai, S. Ishiwata, and Y. Tokura, "Large topological hall effect in a short-period helimagnet mngne," *Phys. Rev. Lett.* **106**, 156603 (2011).
- ¹⁹K. Yasuda, R. Wakatsuki, T. Morimoto, R. Yoshimi, A. Tsukazaki, K. Takahashi, M. Ezawa, M. Kawasaki, N. Nagaosa, and Y. Tokura, "Geometric Hall effects in topological insulator heterostructures," *Nat. Phys.* **12**, 555–559 (2016).
- ²⁰Q. L. He, G. Yin, A. J. Grutter, L. Pan, X. Che, G. Yu, D. A. Gilbert, S. M. Disseler, Y. Liu, P. Shafer, B. Zhang, Y. Wu, B. J. Kirby, E. Arenholz, R. K. Lake, X. Han, and K. L. Wang, "Exchange-biasing topological charges by antiferromagnetism," *Nat. Commun.* **9**, 2767 (2018).
- ²¹D. Zhao, L. Zhang, I. A. Malik, M. Liao, W. Cui, X. Cai, C. Zheng, L. Li, X. Hu, D. Zhang, J. Zhang, X. Chen, W. Jiang, and Q. Xue, "Observation of unconventional anomalous Hall effect in epitaxial CrTe thin films," *Nano Res.* **11**, 3116–3121 (2018).
- ²²B. Ludbrook, G. Dubuis, A.-H. Puichaud, B. Ruck, and S. Granville, "Nucleation and annihilation of skyrmions in Mn₂CoAl observed through the topological Hall effect," *Sci. Rep.* **7**, 1–8 (2017).
- ²³K. K. Meng, X. P. Zhao, P. F. Liu, Q. Liu, Y. Wu, Z. P. Li, J. K. Chen, J. Miao, X. G. Xu, J. H. Zhao, and Y. Jiang, "Robust emergence of a topological Hall effect in MnGa/heavy metal bilayers," *Phys. Rev. B* **97**, 060407 (2018).
- ²⁴L. Zhou, J. Chen, X. Chen, B. Xi, Y. Qiu, J. Zhang, L. Wang, R. Zhang, B. Ye, P. Chen, X. Zhang, G. Guo, D. Yu, J. W. Mei, F. Ye, G. Wang, and H. He, "Topological Hall effect in traditional ferromagnet embedded with black-phosphorus-like bismuth nanosheets," *ACS Appl. Mater. Interfaces* **12**, 25135–25142 (2020).
- ²⁵B. Sohn, B. Kim, J. W. Choi, S. H. Chang, J. H. Han, and C. Kim, "Hump-like structure in Hall signal from ultra-thin SrRuO₃ films without inhomogeneous anomalous Hall effect," *Curr. Appl. Phys.* **20**, 186–190 (2020).
- ²⁶Z. Li, S. Shen, Z. Tian, K. Hwangbo, M. Wang, Y. Wang, F. M. Bartram, L. He, Y. Lyu, Y. Dong, *et al.*, "Reversible manipulation of the magnetic state in SrRuO₃ through electric-field controlled proton evolution," *Nat. Commun.* **11**, 1–9 (2020).
- ²⁷Y. Shiomi, S. Iguchi, and Y. Tokura, "Emergence of topological Hall effect from fanlike spin structure as modified by Dzyaloshinsky-Moriya interaction in MnP," *Phys. Rev. B* **86**, 180404 (2012).
- ²⁸C. Liu, Y. Zang, W. Ruan, Y. Gong, K. He, X. Ma, Q.-K. Xue, and Y. Wang, "Dimensional crossover-induced topological Hall effect in a magnetic topological insulator," *Phys. Rev. Lett.* **119**, 176809 (2017).
- ²⁹T. Kurumaji, T. Nakajima, M. Hirschberger, A. Kikkawa, Y. Yamasaki, H. Sagayama, H. Nakao, Y. Taguchi, T. H. Arima, and Y. Tokura, "Skyrmion lattice with a giant topological Hall effect in a frustrated triangular-lattice magnet," *Science* **365**, 914–918 (2019).
- ³⁰L. Vistoli, W. Wang, A. Sander, Q. Zhu, B. Casals, R. Cichelero, A. Barthélémy, S. Fusil, G. Herranz, S. Valencia, R. Abrudan, E. Weschke, K. Nakazawa, H. Kohno, J. Santamaria, W. Wu, V. Garcia, and M. Bibes, "Giant topological Hall effect in correlated oxide thin films," *Nat. Phys.* **15**, 67–72 (2018).
- ³¹S. Muhlbauer, B. Binz, F. Jonietz, C. Pfleiderer, A. Rosch, A. Neubauer, R. Georgii, and P. Boni, "Skyrmion lattice in a chiral magnet," *Science* **323**, 915–9 (2009).
- ³²C. Pappas, E. Lelièvre-Berna, P. Falus, P. M. Bentley, E. Moskvina, S. Grigoriev, P. Fouquet, and B. Farago, "Chiral paramagnetic skyrmion-like phase in MnSi," *Phys. Rev. Lett.* **102**, 197202 (2009).
- ³³T. Nakajima, H. Oike, A. Kikkawa, E. P. Gilbert, N. Booth, K. Kakurai, Y. Taguchi, Y. Tokura, F. Kagawa, and T. H. Arima, "Skyrmion lattice structural transition in MnSi," *Sci. Adv.* **3**, e1602562 (2017).
- ³⁴X. Z. Yu, Y. Onose, N. Kanazawa, J. H. Park, J. H. Han, Y. Matsui, N. Nagaosa, and Y. Tokura, "Real-space observation of a two-dimensional skyrmion crystal," *Nature* **465**, 901–4 (2010).
- ³⁵S. Seki, X. Z. Yu, S. Ishiwata, and Y. Tokura, "Observation of skyrmions in a multiferroic material," *Science* **336**, 198–201 (2012).

- ³⁶H. S. Park, X. Yu, S. Aizawa, T. Tanigaki, T. Akashi, Y. Takahashi, T. Matsuda, N. Kanazawa, Y. Onose, D. Shindo, A. Tonomura, and Y. Tokura, "Observation of the magnetic flux and three-dimensional structure of skyrmion lattices by electron holography," *Nat. Nanotechnol.* **9**, 337–42 (2014).
- ³⁷S. Heinze, K. Von Bergmann, M. Menzel, J. Brede, A. Kubetzka, R. Wiesendanger, G. Bihlmayer, and S. Blügel, "Spontaneous atomic-scale magnetic skyrmion lattice in two dimensions," *Nat. Phys.* **7**, 713–718 (2011).
- ³⁸A. B. Bogatyrev and K. L. Metlov, "What makes magnetic skyrmions different from magnetic bubbles?" *J. Magn. Magn. Mater.* **465**, 743–746 (2018).
- ³⁹N. Nagaosa and Y. Tokura, "Topological properties and dynamics of magnetic skyrmions," *Nat. Nanotechnol.* **8**, 899–911 (2013).
- ⁴⁰G. Kimbell, P. M. Sass, B. Woltjes, E. K. Ko, T. W. Noh, W. Wu, and J. W. Robinson, "Two-channel anomalous Hall effect in SrRuO₃," *Phys. Rev. Mater.* **4**, 054414 (2020).
- ⁴¹A. Neubauer, C. Pfleiderer, B. Binz, A. Rosch, R. Ritz, P. G. Niklowitz, and P. Böni, "Topological Hall effect in the A phase of MnSi," *Phys. Rev. Lett.* **102**, 186602 (2009).